



Research Article

An experimental study on the impact of porous media in improving the heat transfer performance characteristics of photovoltaic-thermal system

Amjad H. HAMZAWY^{1,*}, Qahtan A. ABED²

¹Engineering Technical College/Najaf, Al-Furat Al-Awsat Technical University, 31001, Iraq

²Technical Institute/Al-Rumaitha, Al-Furat Al-Awsat Technical University, 31001, Iraq

ARTICLE INFO

Article history

Received: 08 November 2023

Revised: 24 April 2024

Accepted: 26 April 2024

Keywords:

Efficiency; Improvement;
Performance; Photovoltaic;
Porous; Thermal

ABSTRACT

Photovoltaic (PV) systems are characterized by their efficiency and performance decreasing as the operating temperature increases. The maximum available tested efficiency of the PV module decreases by up to 0.8% with each 10-degree temperature increase. To perform better PV, it is necessary to extract the heat, and thus decrease its temperature. In the context of this particular research investigation, a series of empirical investigations were conducted at Al-Rumaitha Technical Institute situated in Iraq (31°42' - 45°12'). These experimental endeavors were undertaken to analyze the performance and characteristics of photovoltaic thermal (P^{VT}) collectors. It is noteworthy to mention that one of these solar panels was effectively incorporated into a photovoltaic/thermal (PV/T) module, while the other panel was employed independently without any cooling mechanism. It is essential to underscore that the induction and maintenance of airflow were achieved through the utilization of an air intake fan. It is important to highlight that these experimental investigations were undertaken over a diverse array of days throughout the year, thereby ensuring the thorough coverage of various atmospheric conditions and scenarios. The results show the maximum electrical efficiency achieved was found to be a commendable 19%, representing an impressive improvement of 5.1% when compared to the PV panel without porous. Moreover, it is important to highlight that the maximum output power attained was an astounding 330.7W. Also, the thermal characteristics of the system showed that the maximum amount of heat gain reached a notable 707.1 W. It is also worth noting that the thermal efficiency of the system was calculated to be 29.57%. Lastly, it is pertinent to mention that the overall efficiency of the system, encompassing both electrical and thermal aspects, amounted to an impressive 46.8%.

Cite this article as: Hamzawy AH, Abed QA An experimental study on the impact of porous media in improving the heat transfer performance characteristics of photovoltaic-thermal system. J Ther Eng 2025;11(1):181–195.

*Corresponding author.

*E-mail address: amjed.hamzawy@atu.edu.iq

This paper was recommended for publication in revised form by
Editor-in-Chief Ahmet Selim Dalkılıç



INTRODUCTION

Solar energy can be directly converted into electrical energy by semiconductor solid-state photovoltaic (PV) cells. Most commonly used silicon-based PV cells have an efficiency of around $18\pm 2\%$, but the remaining energy is turned into heat, which raises the temperature of the PV cell [1]. One of the key issues that lower the electrical energy production by 0.4-0.5% is the high temperature of PV panels every 1 C compared to that at 25 °C. Hence, the idea of “PV cooling” emerged as one of the key study areas. Hajibeigy et al. [2] analyzed the thermal response data of a thermal photovoltaic system operating under normal conditions. They used still water as a coolant and examined the heat transfer in each layer of the system. Their research showed that faster heat transfer improves the efficiency of the system. Various methods can be used in the thermal collectors to exchange heat between their layers. These methods may include using rough surfaces like inclined ribs, protrusions, or obstacles. , etc [3, 4]. It's interesting that by reducing the temperature of the surface of a solar cell, it's possible to lower the rate of thermal degradation and increase the efficiency of the cell [5]. An important factor affecting the solar system's electrical efficiency is the usage of a cooling system [6]. Reduced operating temperature increases the solar cell's electrical output and it will be possible to increase overall efficiency [7, 8]. Ahmad et al. [9] reduced the monocrystalline photovoltaic panels' operating temperature. where the exhaust air from the air conditioning units was used to cool the solar panel's backside, the findings revealed an average drop of 18.05 in photovoltaic cells' operating temperature and an 8.65% gain in electrical energy. The electrical efficiency increased by 0.97% as a result. Li et al. [10] researched a technique that uses compressed air to cool and clean solar panels to improve efficiency, and increase the amount of power produced. When adjusting the pumping time at 10, 15, and 20 seconds, the results were an increase in generated energy of 7.30%, 6.33%, and 1.36 %, respectively. Soliman and Hassan [11] presented a study that used experimental data to examine how well photovoltaic cells performed when they were cooled by a heat tube. The heat pipe's condenser was cooled using rectangular fins. The outcomes demonstrated that as the condenser was raised, the cell performance and output power increase as well, where the efficiency grew by 9.1% while the rate of increase in output power was 24.3%. The use of a finned heat sink attached to the back surface of the PV panel increases the heat transfer surface area [12]. Johnston et al. [13] studied the effectiveness of the heat sink in lowering the operating temperature of the solar cells, increasing the output power, and improving efficiency. When the heat sink's fins' height increases, the temperature of the photovoltaic module's back surface drops more quickly. The efficiency was found to have increased by approximately

11.34% and 15.27% at heights of 20 mm and 100 mm, respectively. Some studies have used porous materials and perforated fins to improve heat transfer. For example, Mesgarpour et al. [14] investigated a novel porous heat sink technology that was mounted to the photovoltaic panel, to enhance heat transport and cooling of the solar module. The usage of two horizontal layers, attached to the solar panel's back surface, demonstrated a 15% improvement in heat transfer. Grubišić-Čabo et al. [15] used L-shaped perforated aluminum fins randomly placed on the photovoltaic cell's rear surface. Perforated fins were discovered to provide better cooling and boost efficiency by roughly 2%. The temperature of photovoltaic panels can also be reduced by cooling the front surface of the photovoltaic panel. Bhat et al. [16] Used the front-water cooling technique to enhance 100W solar panel efficiency. The front-cooled water-cooled solar cells achieved an efficiency improvement of 9% with an increase in energy production of 17%.

In this research, the use of porous media heat sinks on the performance of a photovoltaic (PV) module was investigated through a combination of computational fluid dynamics (CFD) and experimental testing. A hybrid system was created using porous metal as a heat sink, it is installed in the form of slanted ribs at a 45-degree angle connected to the back surface of the photovoltaic panel. The main goal is to increase the rate of heat transfer and improve the performance of a photovoltaic unit, and compare it with a reference photovoltaic unit.

MATERIALS AND METHODS

Numerical Configuration

Figure 1 illustrates the design and geometry of a PV module with a heat sink. The heat sink which is made of a porous metal was placed at the back of a solar panel in a zigzag pattern at a 45-degree angle within an air duct. This unique positioning of the heat sink allows for better air circulation around it, thereby enabling it to absorb more heat from the PV panel. The characteristics of PV units are shown in Table 1.

The air duct length is 1984 mm, width is 1007 mm, height is 115 mm, and thickness is 0.7 mm. The air duct was constructed from heavy aluminum, and an insulating material was used to cover the exterior surfaces to shield them from the effects of the environment. The inner surface of the solar panel is covered with a black thermochromic coating to absorb heat to prevent reflection onto the back cell surface. The hole in the porous material has squared dimensions of 1 mm by 1 mm as shown in Figure 2.

The following equations can be used to determine the maximum power generated (P_{mp}) and electrical efficiency (η_e) [17]:

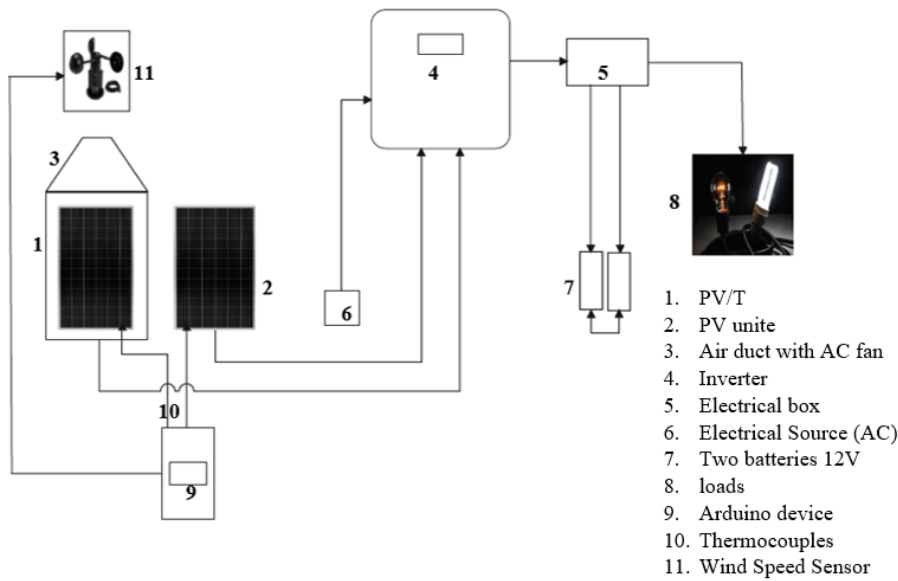


Figure 1. Schematic component PV module.

Table 1. PV Unite characteristics

Details	Characteristics
Type of Solar cell	Mono-crystalline silicon
Maximum Power (Pmax)	375 Wp
The voltage at maximum power (V_{mpp})	40.14 V
Current at maximum power (I_{mpp})	9.35 A
Open circuit voltage (V_{oc})	48.67 V
Short circuit current (ISC)	9.94 A
Panel efficiency	19.75%
Standard test conditions	Air mass 1.5, radiation 1000 W/m ² , at 25°C
Number of cells	72
Panel Dimensions (H/W/D)	1984x1007x40 mm
Weight	22.5 kg
Range of operating temperatures	-40-85°C

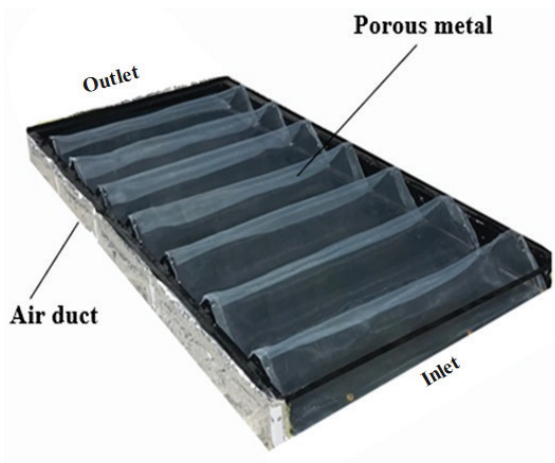


Figure 2. Air duct with porous media.

$$P_{mp} = V_{mp} \cdot I_{mp} \tag{1}$$

$$\eta_e = \left(\frac{P_{mp}}{G \cdot A_{pv}} \right) * 100 \tag{2}$$

Where (V_{mp}) and I_{mp} are the maximum voltage and maximum current respectively, (G) is the intensity of solar radiation (W/m^2), and (A_{pv}) is the active area of the PV panel (m^2). The electrical efficiency of solar cells is also calculated as a function of temperature through the following equation [18]:

$$\eta_e = \eta_0 [1 - \beta(Tc - Ta)] \tag{3}$$

Where (η_0) is nominal efficiency, β is the temperature coefficient ($0.0045^\circ C^{-1}$), Tc is the cell temperature ($^\circ C$), and Ta is the ambient temperature ($^\circ C$).

The purpose of the simulations was to investigate how actual weather affects a two-dimensional model. COMSOL Numerical was utilized to generate the monocrystalline model that was employed in the simulations. The solar panel collector is divided into four isothermal zones for the simulation model: the front region contains the PV glass cover, the photovoltaic cells, the Ethyl Vinyl Acetate (EVA) which is a layer that covers solar cells, and the back PV cover, followed by the screen heat absorber, and the air duct which is the final section, as can be seen in Figure 3. The geometry and grid (mesh) were generated by COMSOL. Various mesh types were studied using three different sizes - normal, coarse, and fine to accommodate the different sizes of the model parts, as can be seen in Figure 4.

Experimental Work

The electrical performance of the PV/T system used in this study was investigated. The module is set on the rooftop of Al-Rumaitha Technical Institute in Al-Muthana, Iraq ($31^{\circ}42' - 45^{\circ}12'$) / Al-Furat Al-Awsat Technical University. The study was conducted to determine how the operating temperature of the PV module impacted its efficiency.

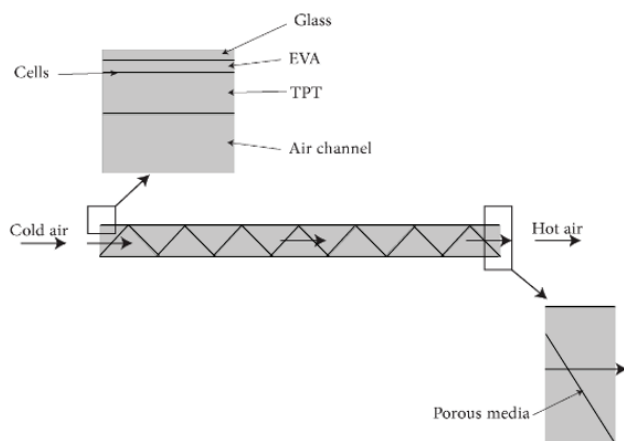


Figure 3. 2-D COMSOL model displays the main structure of PV/T.

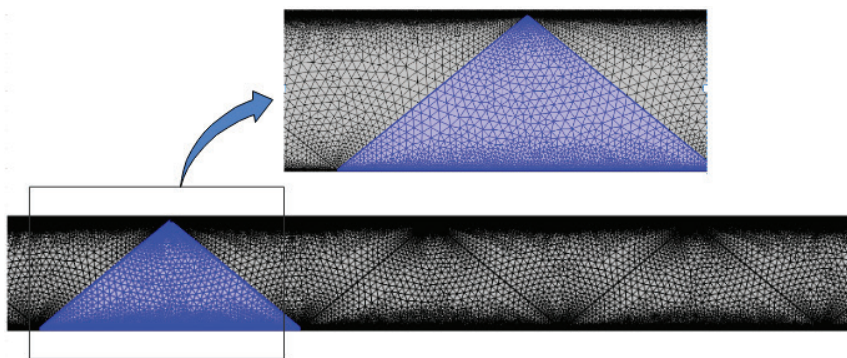


Figure 4. 2-D Front view of meshed PV/T system with porous media.

These are two photovoltaic panels with a power of 375 W. One of the panels was mounted on the module that cooled the PV panel to compare the performance with the other panel without cooling. The air duct allows air to pass under the PV panel using an AC air fan placed above the air duct. The porous metal (metal grid) is fitted within the air duct in the shape of a zigzag at an angle of 45° as shown in Figure 5. To improve the heat transfer from the solar cells to the air passing through the porous media, it is connected to the back surface of the solar panel at a distance of 20 mm. The porous media is made of iron metal with an opening area of $1\text{ mm} \times 1\text{ mm}$.

The necessary data in this testing process were recorded using several devices, including the Solar Power Meter device to measure the intensity of solar radiation. The Arduino device was used to record the temperatures of the front and back surfaces of the photovoltaic panels, the temperature of the incoming and outgoing air through a K-type sensor and thermocouple connected to the Arduino, the ambient temperature, and the air speed through the air-speed sensor. Figure 6 shows the parts of the devices used for measurement. The characteristics of the measuring devices and sensors are presented in Table 2. The final appearance of the photovoltaic thermal system can be seen in Figure 7.

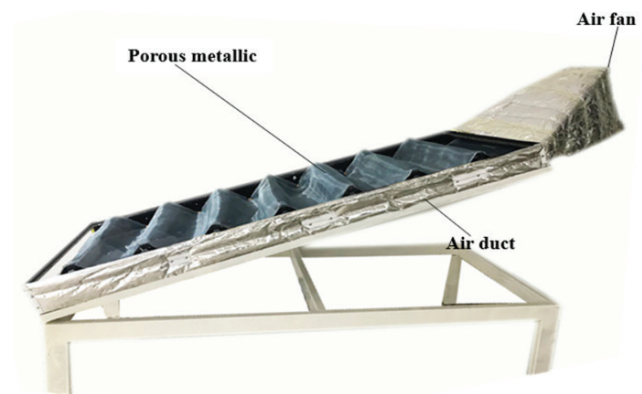


Figure 5. Air duct with fan.



Figure 6. Measuring devices: a) Component Arduino b) Solar power meter c) Arduino device.

Table 2. The characteristics of measuring devices and sensors

Device	Model	Accuracy	Resolution
Solar power meter	SM206-Solar	$\pm 10\text{W/M}^2$	0.1W/M^2 , $0.1\text{ BTU}/(\text{FT}^2\text{-H})$
Ambient temperature and Humidity sensor	DHT22	humidity $\pm 2\%$ RH (Max $\pm 5\%$ RH); temperature $< \pm 0.5^\circ\text{C}$	humidity 0.1% RH; temperature 0.1°C
Temperature sensor	MAX6675	$\pm 3^\circ\text{C}$	0.25°C
Wind speed sensor	IP65 grade	$\pm 3\%$	0.1m/s
Thermocouple	K-type	$\pm 1.5^\circ\text{C}$	



Figure 7. Experimental setup of the PV unit and PV/T system.

Economic Analyses

The cost analysis of the solar system is very necessary to judge the performance of the system and know the economic feasibility, as shown in Table 3. The following are the calculation procedures [19]:

Average yield per year/m² = Average daily yield /m² * 365.

The Capital Recovery Factor (CRF) is calculated by:

$$CRF = \left(\frac{r(1+r)^n}{(1+r)^n - 1} \right) \quad (4)$$

where r is the annual rate of interest which is 10% and n is the number of the useful years where the still can work and it is proposed 10 years the first annual cost (FAC) is given by:

$$FAC = CRF * P \quad (5)$$

where P is the initial cost. The sinking fund factor (SFF) for a system is governed by:

$$SFF = \left(\frac{r}{(1+r)^n - 1} \right) \quad (6)$$

The salvage value (S) is assumed as 50% of the first annual cost and the annual salvage value (ASV) is computed by:

$$ASV = SFF * S \quad (7)$$

Table 3. Cost analysis of the solar system

Material	Cost	Power Cost \$/W
PV Panel	250 \$	
Air duct	100 \$	
Porous metal	15 \$	7.05
Air fan	30 \$	
Metal structure	75 \$	
Total cost	470 \$	

That the Annual Maintenance Cost (AMC) will be 15% of the first year's cost.

Annual cost (AC) = Initial annual cost + Annual maintenance cost - annual salvage value.

RESULTS AND DISCUSSION

COMSOL Simulation Results

The air channel has been analyzed to obtain the best heat exchange between the base of the photovoltaic panel and the air, by changing the number of porous metal ribs inside the air duct, where the simulation process is done depending on the number of different ribs 10, 12, and 14, ribs as shown in Figure 8. The results show that the best design is using 14 ribs at an angle of 45°.

Figure 9 shows the change in the surface temperature of the photovoltaic panel during the cooling time. From the figure, it can be seen that the temperature increases over

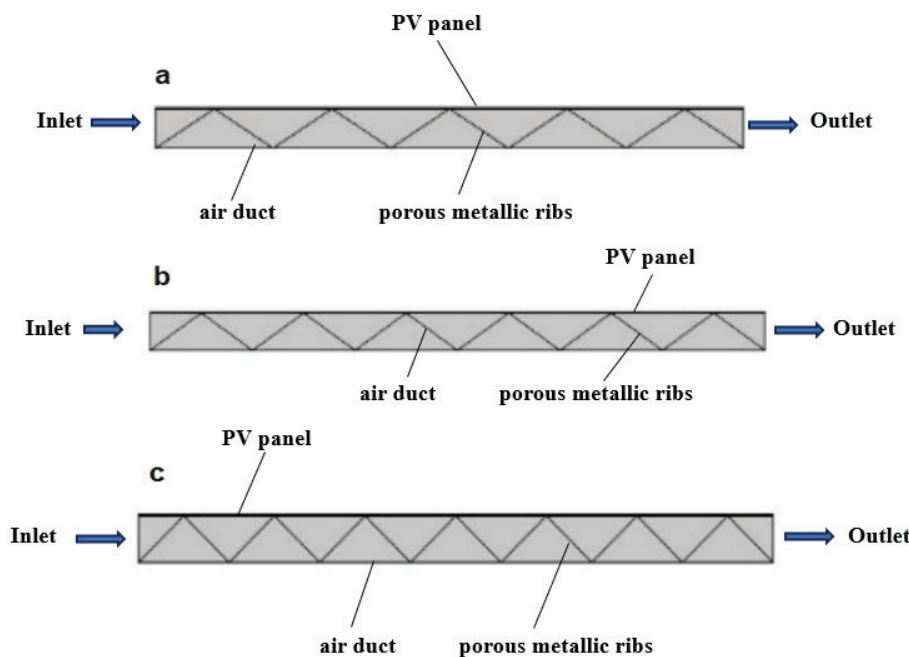


Figure 8. Number of porous metallic ribs a)10 ribs b)12 ribs c) 14 ribs.

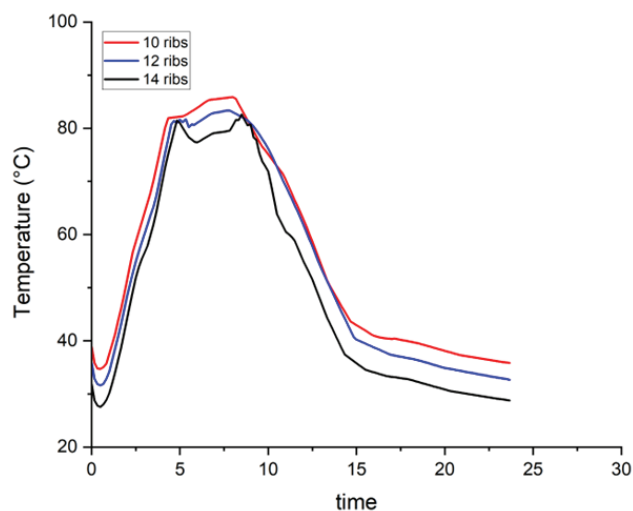


Figure 9. Varies surface temperature of PV panels with different number of ribs porous media.

time. It can be also noticed that the temperature of the photovoltaic panel varies according to the number of porous metal ribs. By increasing the number of ribs, the operating temperature of photovoltaic panels decreases so the average temperatures of the surface PV panels for the cases of 10 ribs, 12 ribs, and 14 ribs are 56.2°C, 53.9°C, and 49.7°C, respectively.

A side view of the PV/T system simulation is shown in Figure 10, where the temperature distribution can be observed in the proposed module. It is noted that the operating temperature of the photovoltaic module increases with the intensity of solar radiation until it reaches up to 82°C after 6.8 hours of cooling during the simulation process. Due to the heat exchange between the photovoltaic panel, the metal grid, and the air, it can be seen that the temperature inside the air duct increases in the direction of the airflow.

The COMSOL Multiphysics model was simulated to compute the streamline air velocity, temperature distribution, and pressure drop in the 2D of the PV/T system. Figure 11a presents the streamline velocity of air flowing through the triangular screen. The air temperature distribution inside the air duct for the PVT air collector has been illustrated in Figure 11b. The simulation result clarifies an increase in air temperature near the cell. The leaving air temperature has been increased from 319 K to 329 K by using porous metal. Figure 11c illustrates the pressure distribution inside the air duct, it was the highest value in perforations.

From Figure 12 it can be seen that there is a substantial effect depending on how many ribs of the porous material are in contact with the PV panel's rear surface. By increasing the number of ribs, the surface area of the heat sink increases, and efficiency also increases. The more ribs there are the better the heat transfer. Based on the findings, in this study, it can be observed the efficiency rate varies

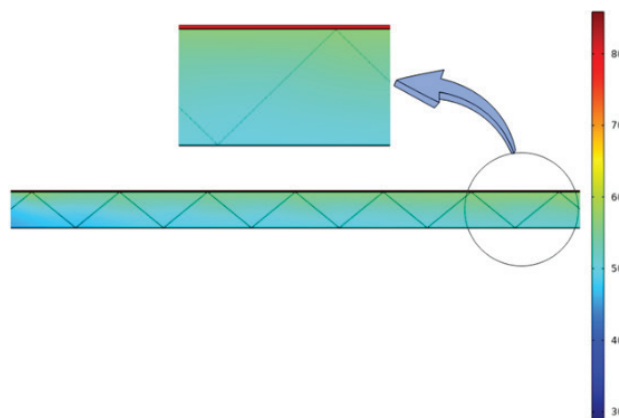


Figure 10. Side view of the PV/T system simulation after 6.8 hours of cooling.

depending on the number of ribs used. Specifically, have been found that using 10 ribs resulted in an efficiency rate of 16.6%, while using 12 ribs increased the rate to 17%, and using 14 ribs further improved the efficiency rate to 17.7%. This represents an overall rate of improvement of 4.2%.

Experimental Results

Figure 13 shows climate changes for several days, solar radiation, and ambient temperature during the hours of the day. At the beginning of the experimental work, the lowest solar radiation was at a rate of 267.42 W/m² at 8:00 am, and the ambient temperature was 36.78°C. As it kept rising the greatest readings were noted at 1:10 pm. The rate of ambient temperature was 46.2 °C, and the rate of irradiance was 1189.2 W/m².

According to Figure 14, there is a correlation between the temperature of the photovoltaic panel and the intensity of solar radiation. As the solar radiation increases, the temperature of the panel also rises. This information can be useful in understanding the behavior of photovoltaic panels under different weather conditions and can aid in optimizing their efficiency. According to the recorded data, it was observed that at the lowest intensity of solar radiation, which was 250.5 W/m², the temperature of the photovoltaic cell reached 46°C. However, as the solar radiation increased and reached the maximum level of 1214.7 W/m², the temperature of the solar cell also increased and reached 69°C. It is important to monitor and regulate the temperature of the solar cell to ensure its optimal performance and longevity.

The effect of cooling on the temperature of photovoltaic (PV) panels is very important. It is necessary to understand how cooling can impact the performance and efficiency of these panels to ensure they function at their best. During working days on the experiment, three different air mass flow rates to cool down thermal PV/T system were tested. These air mass flow rates were 0.057kg/s, 0.096/s, and 0.111kg/s. Figure 15 represent the average temperatures of photovoltaic cells with and without a cooling system. The

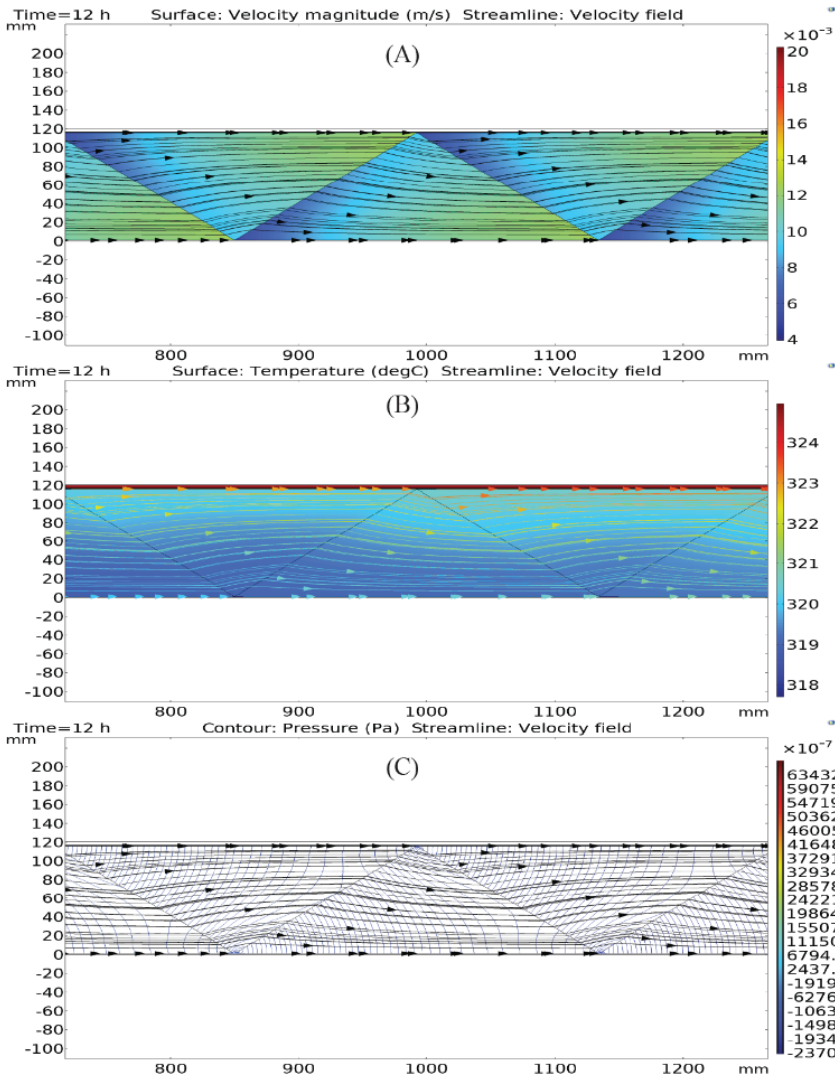
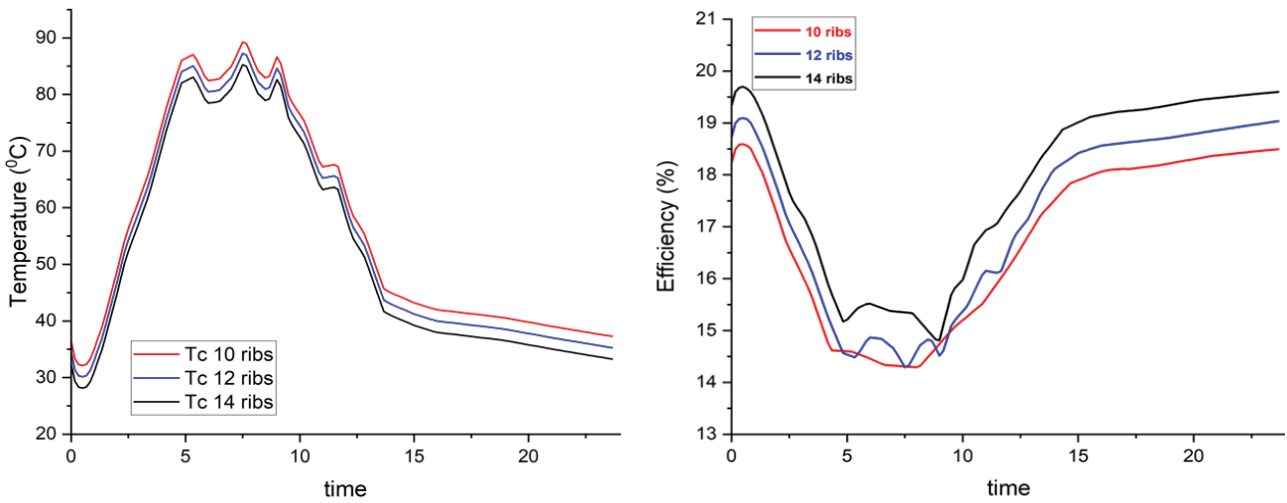


Figure 11. Evaluation of air inside the duct a) Streamline velocity, b) Air temperature distribution and c) Pressure drop.



a) b) Figure 12. a) PV/T efficiency depending on the number of porous metal ribs b) PV temperature depending on the number of porous metal ribs.

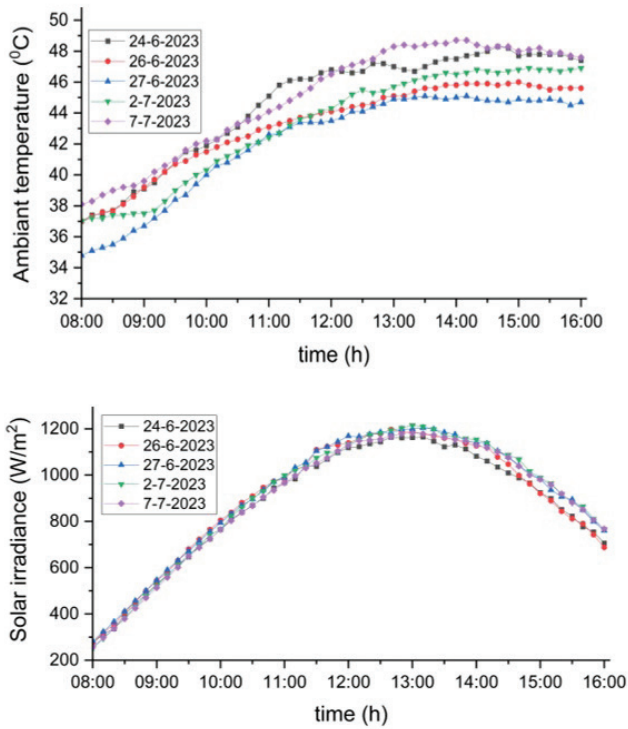


Figure 13. Variations of ambient temperature and solar radiation for several days.

results clearly show that the panel with cooling experienced significantly lower temperatures. On June 27, 2023, at an air mass flow rate of 0.111kg/s, the average temperature of the cooled panel was 49.5°C with a maximum temperature of 56.25°C, while the panel without cooling had an average temperature of 56.9°C with a maximum temperature of 62.37°C. This represents a temperature decrease of approximately 15.7%.

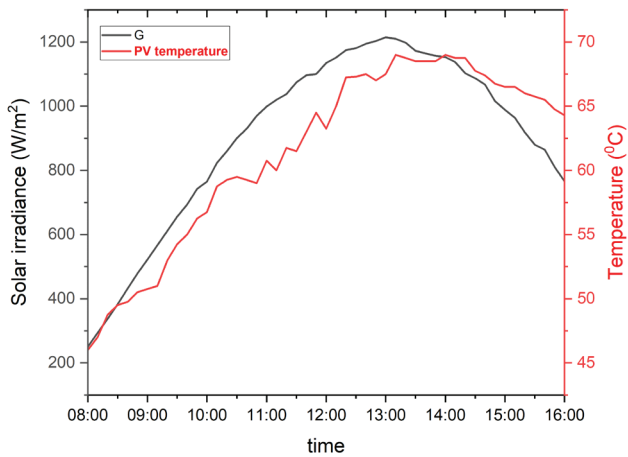


Figure 14. PV module temperature and solar radiation 5th June 2023.

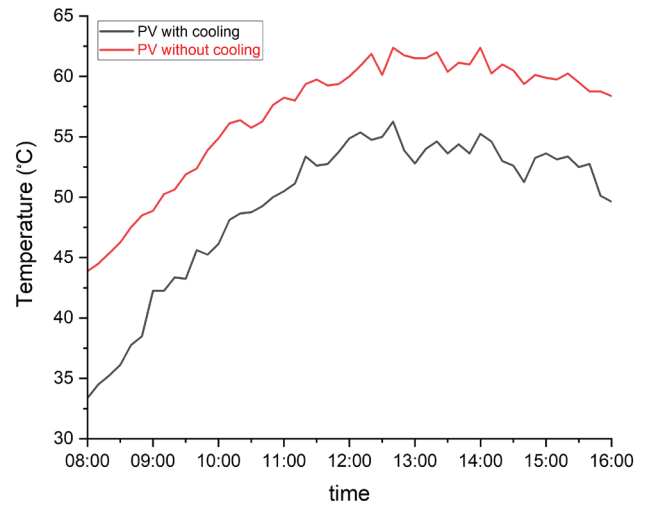


Figure 15. PV panels temperature with and without cooling 27th June 2023.

Based on the data presented in Figure 16 it was found that the current difference between PV panels with and without cooling is very small, with a recorded average difference of 0.07 A. The two panels' units with and without cooling recorded a maximum current of 8.1A, and 8.78A, respectively. It was also noted that during the final hours of the experiment, both units recorded nearly identical current levels as a result of the decrease in solar radiation. and temperature.

From Figure 17 it can be seen that there is a clear correlation between temperature and the voltage of the PV panel. At the start of the experiment, the photovoltaic panel's voltage was higher due to lower temperatures and higher relative humidity. However, as the temperature increased

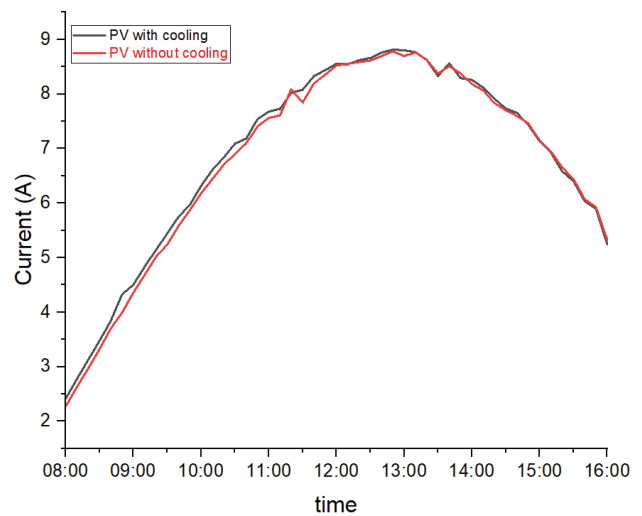


Figure 16. Current PV with and without cooling 24th June 2023.

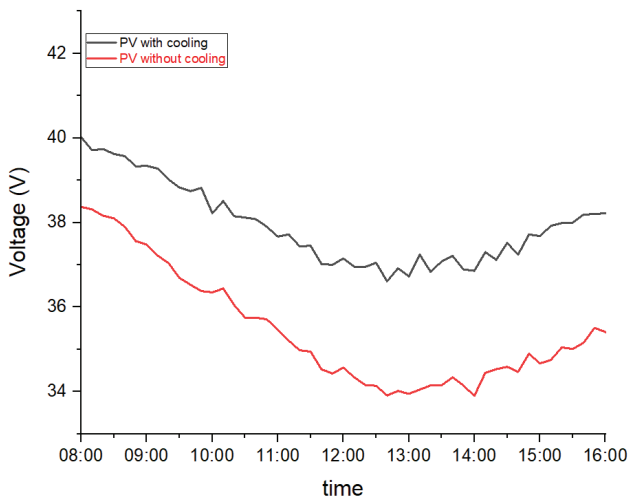


Figure 17. Voltage PV with and without cooling 7th July 2023.

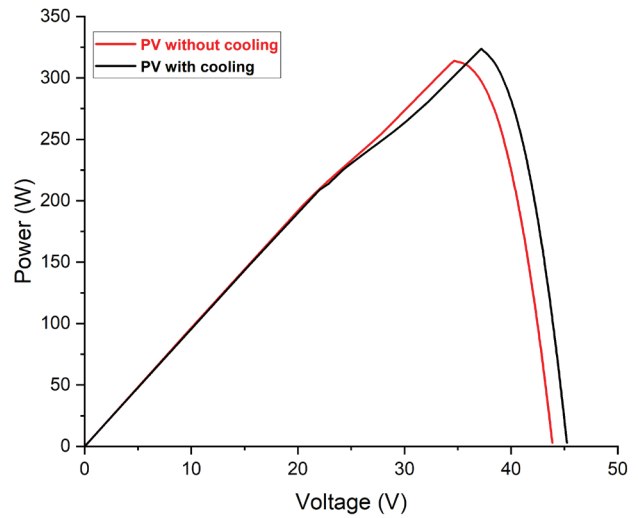


Figure 19. P-V curve for PV with and without cooling 5th June 2023.

and humidity decreased, the voltage gradually declined. With the implementation of cooling, the average voltage increased by 2.47, as the PV panel with cooling yielded an average voltage of 37.93V, compared to the reference panel which recorded an average voltage of 35.46V. Thus, the level of improvement in voltage is 6.9%.

Figure 18 shows a comparison of the output power of two PV panels, with and without cooling. The findings indicate that at 1:00 PM, panels had the highest output power, the PV unit with cooling producing 330.7W and the unit without cooling producing 314W. This confirms the effectiveness of the cooling technique, as the unit with cooling consistently produced higher output power throughout the experiment. It is worth noting that the output power showed an improvement rate of approximately 5%, which

was expected as it depends on factors such as airspeed and surrounding temperature.

Looking at the performance curves for current and output power versus voltage, I-V curve, and P-V curve, in Figures 19 and 20, it is interesting to note the differences in output power and current versus voltage between a solar PV/T system with cooling and a PV module without cooling. At the highest solar radiation value considered ($G = 1214.7 \text{ W/m}^2$), the output power of the PV/T system with cooling is 323 W, while the output of the PV module without cooling is only 313 W. In the case of current, the improvement or difference is usually very small between the panels with and without cooling. Through the results, it can be seen that the proposed cooling technology enhances

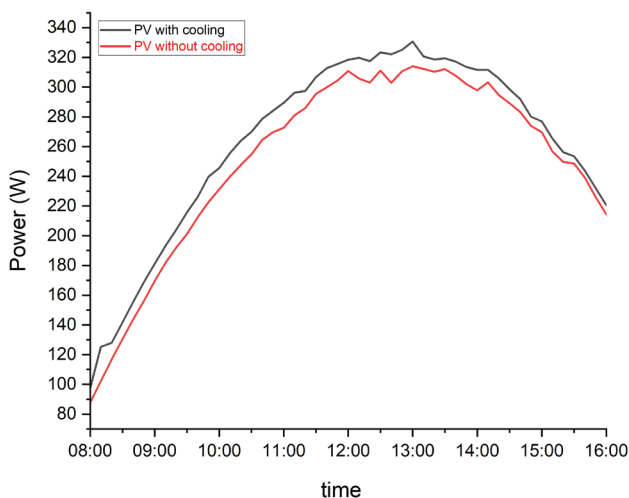


Figure 18. Power PV with and without cooling 27th June 2023.

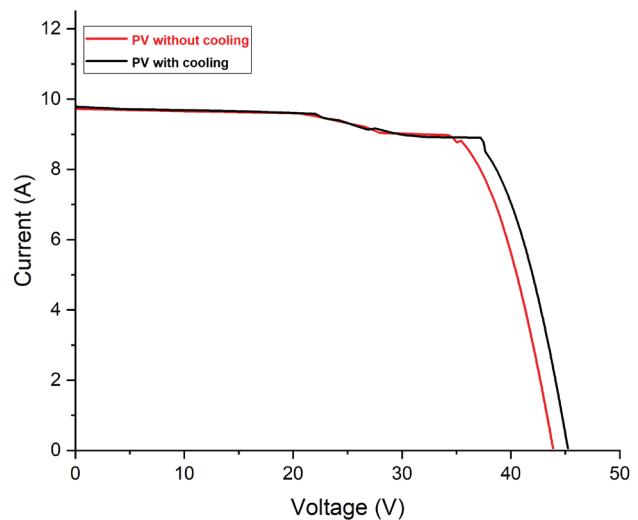


Figure 20. I-V curve for PV with and without cooling 5th June 2023.

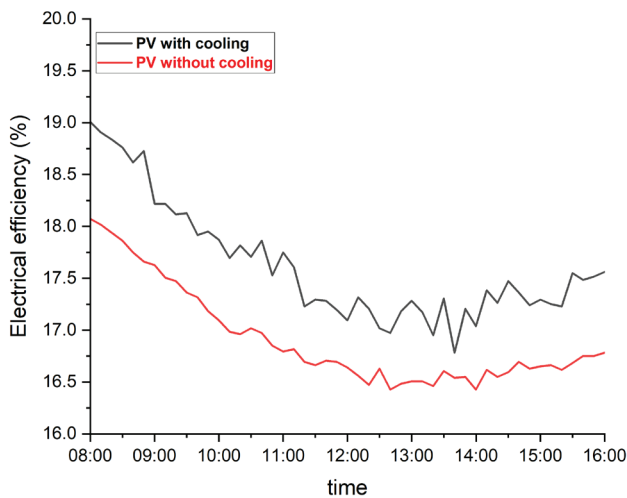


Figure 21. Electrical efficiency with and without cooling 27th June 2023.

the output power and current when compared with the reference panel.

In this study, it has been compared the efficiency of a photovoltaic panel with and without cooling over a period, which was calculated by Equation 3 as shown in Figure 21. The results showed that as temperatures increased due to higher solar radiation intensity, the performance of the panel decreased. Specifically, for every 10 °C increase in temperature, the electrical efficiency decreased by 0.8%. However, based on the research conducted in this study, it was found that by applying a cooling technique, the efficiency of the panel increased by 5.1% compared to the reference panel. The average electrical efficiency for panels with and without cooling was 17.61% and 16.9%, respectively. These findings suggest that cooling can be an effective way to improve the efficiency of photovoltaic panels.

Figure 22 depicts the change in heat transfer rate due to variations in solar intensity. It can be seen that as solar radiation increases, the temperature rises, increasing the amount of heat gained. At the experiment's start, 63.9 W of heat was gained with a solar irradiance of 273.2 W/m². It rises as the solar intensity rises until it reaches its maximum of 380.3 W at 1164.8 W/m² of solar radiation. Figure 23 depicts the change in thermal efficiency rate due to variations in solar intensity. It can be seen that as solar radiation increases, the temperature rises, increasing the amount of thermal efficiency. At the experiment's start, 11.7 % of thermal efficiency with a solar irradiance of 273.2 W/m². It rises as the solar intensity rises until it reaches its maximum of 20.6 % at 1164.8 W/m² of solar radiation.

The results that can be seen from Figure 24 show that the overall efficiency rate of the system is 43% with a maximum overall efficiency value of 46.8%.

The impact of increasing the flow rate on the electrical efficiency of the PV panels is shown in Figure 25. The results indicated that increasing the flow rate improves the

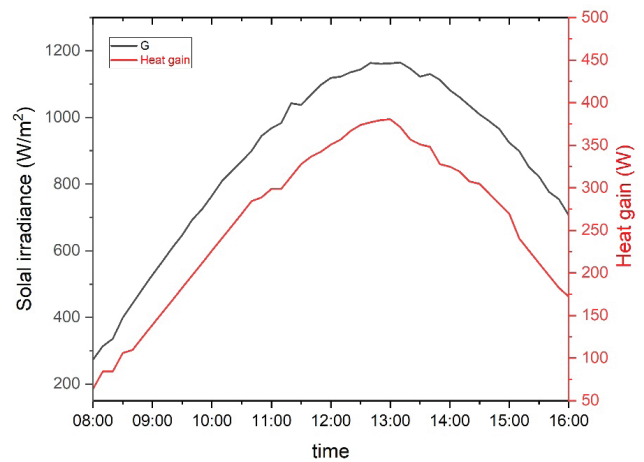


Figure 22. Heat gain and solar radiation 24th June 2023.

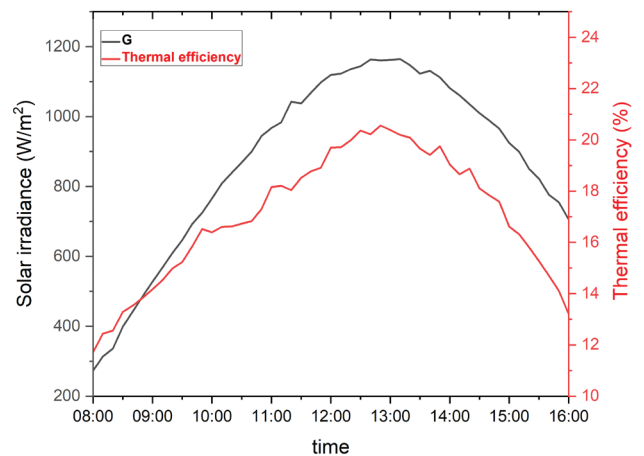


Figure 23. Thermal efficiency and solar radiation 24th June 2023.

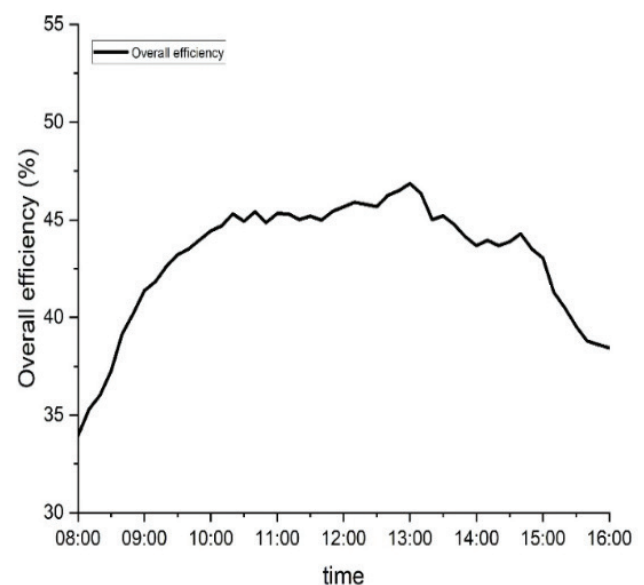


Figure 24. Overall efficiency of PV/T module 27th June 2023.

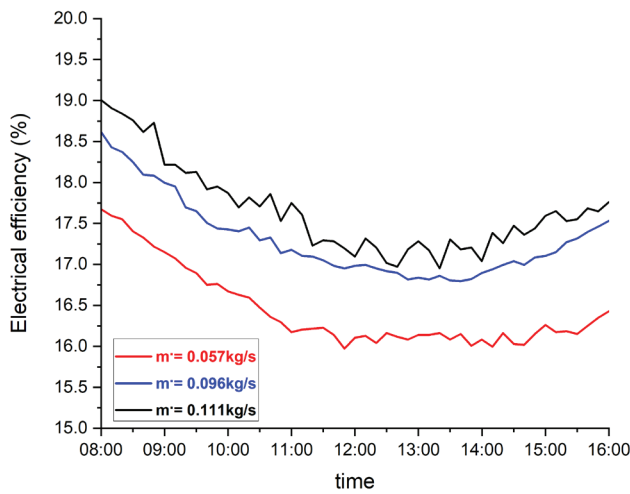


Figure 25. Electrical efficiency for PV/T unit with various mass flow rates.

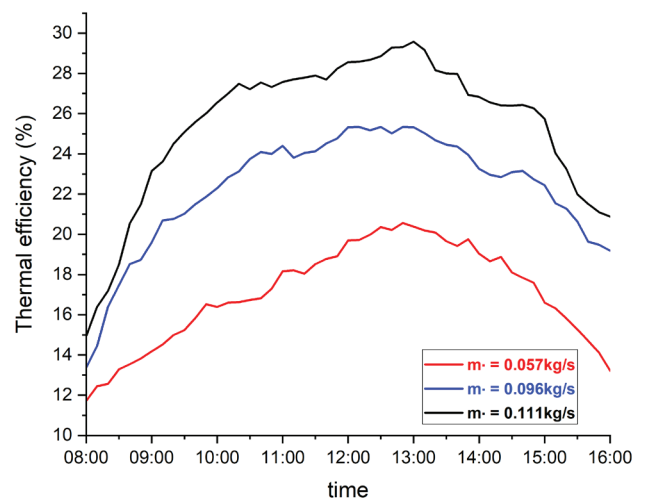


Figure 27. Thermal efficiency with various mass flow rates.

efficiency of the proposed technology for cooling PV panels, whereby the operating temperature of the photovoltaic cells decreases, which positively affects the performance of the PV/T module. The results recorded for the average efficiency for the 0.057 kg/s, 0.096 kg/s, and 0.111 kg/s cases, were 16.17%, 17.06%, and 17.43% with an improvement rate of 2.3%, 2.9%, and 4.13%, respectively.

Figure 26 shows the effect of the change in the mass flow rate on the amount of heat gained. Increasing the air mass flow rate increases the heat gained from the thermal photovoltaic system. The findings showed that the biggest quantity of heat gain, in the amount of 701.6 W, could be obtained at the highest flow rate of 0.111 kg/s, compared with the other two cases, 0.057 kg/s, and 0.096 kg/s, where the results were 380.3 W and 600.5 W.

Thermal efficiency increases with an increase in the air mass flow rate. Figure 27 shows a comparison between

the three cases, where it can be seen that the highest rate of thermal efficiency was obtained 25.4% for a mass flow rate of 0.111 kg/s. Compared to the other two cases 0.057 kg/s and 0.096 kg/s, the average thermal efficiency was 17% and 22.2%, respectively. The comparison of electrical and thermal efficiency can be seen in the Figure 28 with a mass flow rate of 0.111. It was noted that the highest value of thermal efficiency at 1:00 pm was about 28.8%, while the lowest value of electrical efficiency was about 16.9%.

Figure 29 shows the comparison of the total efficiencies between three cases of mass flow rates 0.057 kg/s, 0.096 kg/s, and 0.111 kg/s, for the PV/T system. As a result of increasing the electrical and thermal efficiency of the proposed system in response to the increase in flow rates, the overall efficiency of the system increases. The results showed that the maximum total efficiency for the three cases was 36.8%, 42.4%, and 46.8%, respectively.

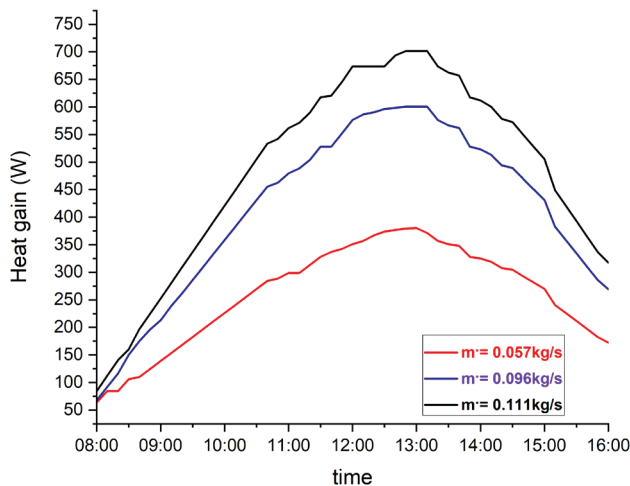


Figure 26. Heat gain with various mass flow rates.

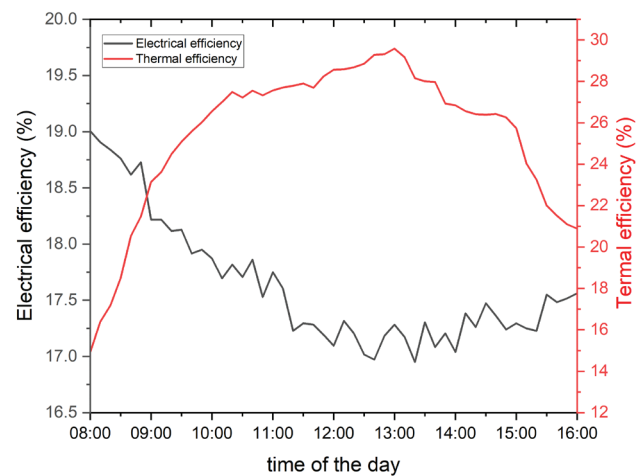


Figure 28. Comparison between electrical and thermal efficiency.

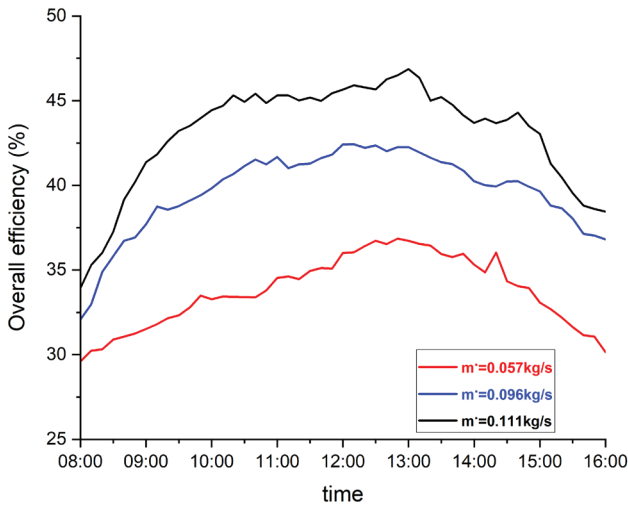


Figure 29. Overall efficiency with various mass flow rate.

In Figure 30, a comparison is shown between the output power and efficiency during the experimental working days. It is worth noting that the highest values were achieved on the 26th and 27th of June, where the maximum power reached 326.8 watts and 330.7 watts respectively. The

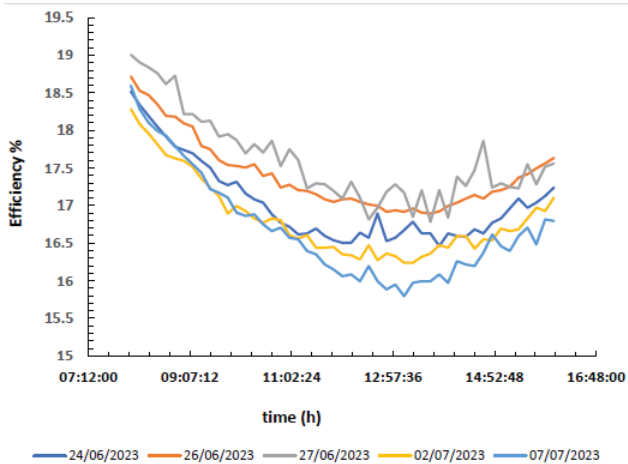
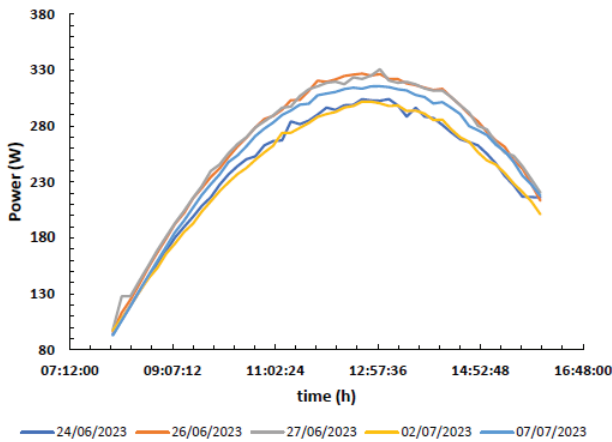


Figure 30. Comparison of output power and efficiency for the experimental working days.

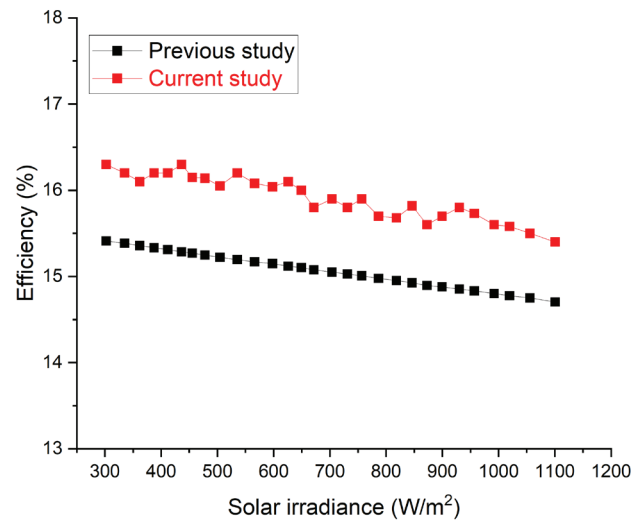


Figure 31. Comparison the efficiency with previous.

maximum efficiency for those days was 18.7% and 19% respectively.

Comparison of Experimental Results with a Previous Study

The findings were compared to one of the previous studies [20], as illustrated in Figure 31. The graph demonstrates a comparison between the electrical efficiency of the previous study and the current study, as well as its response to solar radiation. The results were so good, as the percentage difference between them was only 5.57% studies.

CONCLUSION

The hybrid PV/T system generates both thermal and electrical energy, and the active cooling mechanism was found to have a significant impact based on experimental results. Where the air-cooled PV / T thermal photovoltaic system using porous metal media is a practical and economical technique for reducing the operating temperature of PV panels and increasing their performance and efficiency. The air was applied to the back surface of the photovoltaic panel within the air duct, which contains the porous metal attached to the back surface of the photovoltaic panel. The effect of increasing the number of porous metal ribs and the mass flow rate of air on the heat exchange and improving the performance of the photovoltaic panel was also studied. By comparing it with the plate without cooling, the following conclusions were obtained:

1. The environmental factors that affect the performance of the thermal photovoltaic system are the intensity of solar radiation, the ambient temperature, and the humidity level.
2. It is necessary to control the amount of air mass flow rate because it improves the performance of the photovoltaic

module and increases its thermal and electrical efficiency. The highest results were obtained at a flow rate of 0.111 kg/s.

3. The rate of decrease in the base temperature of the photovoltaic panel reached 17%. Where the average temperature decreased at the highest air mass flow rate from 9.56 °C to 49 °C. Thus, the electrical efficiency and output power are significantly increased.
4. The average electrical efficiency obtained after the cooling process of the PV/T system is 17.63% with a maximum electrical efficiency of 19% from the nominal efficiency of the photovoltaic panel of 19.75%. An improvement rate for electrical efficiency is 6.9%.
5. The maximum output power of the PV/T system after cooling was 330.6W compared to 314W for the PV module without cooling. The net gain at the output power is 16 W with the rate of improvement in output power is 5%.
6. The maximum heat gain from the PV / T system is 701.6 W at the highest air mass flow rate.
7. The maximum thermal efficiency of the PV / T system reached 29.57% by using porous metal media inside the air duct. This is due to the difference between the temperature of the air entering and leaving the airway of 6.25.

Regarding future studies, we suggest using the hot air produced by the PV/T system in different applications such as drying agricultural crops. It is also possible to cool the front surface of the photovoltaic panel using water spray, in addition to cooling the back surface to ensure better cooling and clean the front surfaces of dirt and dust.

NOMENCLATURE

Symbol	
PV	Photovoltaic
PV/T	Photovoltaic thermal
DC	Constant current, A
A	Area of PV panel, m ²
AC	Alternating current, A
PPFHS	Plate pin fin heat sink
PFHS	Plate fin heat sink
TMS	Thin metal plates suspended
CFD	Computational fluid dynamic
T _{pv}	Photovoltaic temperature, °C
PMP	Maximum power point, W
G	Solar irradiance, W/m ²
V _w	Wind speed, m/s
T _{amb}	Ambient temperature, °C
P _m	Maximum power, W
I _m	Maximum current, A
V _m	Maximum voltage, V
FF	Fill factor
I _{sc}	Short circuit current, A
V _{oc}	Open circuit voltage, V
η _{cel}	PV efficiency, %

η _{Tref}	Electrical efficiency at T _{ref} %
β _{ref}	Temperature coefficient (0.0045), k ⁻¹
S	PV cell temperature, °C
T _{ref}	PV reference temperature, °C
Q _u	Heat gained, W
\dot{m}	Mass flow rate, Kg/s
cp	Specific heat, kJ/kg K
ΔT	Difference of incoming and outgoing temperatures, °C
η _{th}	Thermal efficiency %
η _O	Overall efficiency %
ρ	Density of air, Kg/m ³
RMSE	Root mean square error
M	Total quantity of values for the efficiency

AUTHORSHIP CONTRIBUTIONS

Authors equally contributed to this work.

DATA AVAILABILITY STATEMENT

The authors confirm that the data that supports the findings of this study are available within the article. Raw data that support the finding of this study are available from the corresponding author, upon reasonable request.

CONFLICT OF INTEREST

The authors declared no potential conflicts of interest with respect to the research, authorship, and/or publication of this article.

ETHICS

There are no ethical issues with the publication of this manuscript.

REFERENCES

- [1] Zhao Y, Gong S, Zhang C, Ge M, Xie L. Performance analysis of a solar photovoltaic power generation system with spray cooling. *Case Stud Therm Eng* 2022;29:101723. [\[CrossRef\]](#)
- [2] Hajibeigy MT, Walvekar R, CV A. Mathematical modelling, simulation analysis of a photovoltaic thermal system. *J Therm Eng* 2021;7:291–306. [\[CrossRef\]](#)
- [3] Bisht YS, Pandey SD, Chamoli S. Jet impingement technique for heat transfer enhancement: Discovering future research trends. *Energy Sources Part A Recover Util Environ Eff* 2023;45:8183–8202. [\[CrossRef\]](#)
- [4] Bisht YS, Pandey SD, Chamoli S. Experimental investigation on jet impingement heat transfer analysis in a channel flow embedded with V-shaped patterned surface. *Energy Sources Part A Recover Util Environ Eff* 2023;45:12520–12534. [\[CrossRef\]](#)

- [5] Shalaby SM, Elfakharany MK, Moharram BM, Abosheisha HF. Experimental study on the performance of PV with water cooling. *Energy Rep* 2022;8:957–961. [\[CrossRef\]](#)
- [6] Shoeibi S, Kargarsharifabad H, Mirjalily SAA, Zargarazad M. Performance analysis of finned photovoltaic/thermal solar air dryer with using a compound parabolic concentrator. *Appl Energy* 2021;304:117778. [\[CrossRef\]](#)
- [7] Dwivedi P, Sudhakar K, Soni A, Solomin E, Kirpichnikova I. Advanced cooling techniques of P.V. modules: A state of art. *Case Stud Therm Eng* 2020;21:100674. [\[CrossRef\]](#)
- [8] Salameh W, Castelain C, Faraj J, Murr R, El Hage H, Khaled M. Improving the efficiency of photovoltaic panels using air exhausted from HVAC systems: Thermal modelling and parametric analysis. *Case Stud Therm Eng* 2021;25:100940. [\[CrossRef\]](#)
- [9] Ahmad FF, Ghenai C, Hamid AK, Rejeb O, Bettayeb M. Performance enhancement and infra-red (IR) thermography of solar photovoltaic panel using back cooling from the waste air of building centralized air conditioning system. *Case Stud Therm Eng* 2021;24:100840. [\[CrossRef\]](#)
- [10] Li D, King M, Dooner M, Guo S, Wang J. Study on the cleaning and cooling of solar photovoltaic panels using compressed airflow. *Sol Energy* 2021;221:433–444. [\[CrossRef\]](#)
- [11] Soliman AMA, Hassan H. An experimental work on the performance of solar cell cooled by flat heat pipe. *J Therm Anal Calorim* 2021;146:1883–1892. [\[CrossRef\]](#)
- [12] Nehari T, Benlakam M, Nehari D. Effect of the fins length for the passive cooling of the photovoltaic panels. *Period Polytech Mech Eng* 2016;60:89–95. [\[CrossRef\]](#)
- [13] Johnston E, Szabo PSB, Bennett NS. Cooling silicon photovoltaic cells using finned heat sinks and the effect of inclination angle. *Therm Sci Eng Prog* 2021;23:100902. [\[CrossRef\]](#)
- [14] Mesgarpour M, Heydari A, Wongwises S, Reza Gharib M. Numerical optimization of a new concept in porous medium considering thermal radiation: Photovoltaic panel cooling application. *Sol Energy* 2021;216:452–467. [\[CrossRef\]](#)
- [15] Grubišić-Čabo F, Nižetić S, Čoko D, Marinić Kragić I, Papadopoulos A. Experimental investigation of the passive cooled free-standing photovoltaic panel with fixed aluminum fins on the backside surface. *J Clean Prod* 2018;176:119–129. [\[CrossRef\]](#)
- [16] Bhat P, Iyengar AS, Abhilash N, Reddy PK. Experimental investigation and validation of solar PV cooling for enhanced energy conversion efficiency for Indian climatic conditions. *J Therm Eng* 2022;8:711–718. [\[CrossRef\]](#)
- [17] Choubineh N, Jannesari H, Kasaeian A. Experimental study of the effect of using phase change materials on the performance of an air-cooled photovoltaic system. *Renew Sustain Energy Rev* 2019;101:103–111. [\[CrossRef\]](#)
- [18] Teo HG, Lee PS, Hawlader MNA. An active cooling system for photovoltaic modules. *Appl Energy* 2012;90:309–315. [\[CrossRef\]](#)
- [19] Abd Elbar AR, Hassan H. An experimental work on the performance of new integration of photovoltaic panel with solar still in semi-arid climate conditions. *Renew Energy* 2020;146:1429–1443. [\[CrossRef\]](#)
- [20] Abudllah Y, Arifin Z, Prija Tjahjana DD, Suyitno S, Putra MRA. Analysis of the copper and aluminum heat sinks addition to the performance of photovoltaic panels with CFD modelling. *Proceeding - 1st Int Conf Inf Technol Adv Mech Electr Eng ICITAMEE 2020* 2020:41–45. [\[CrossRef\]](#)